Energy and Time Characterization of Silicon Photomultiplier Detector Blocks

Sahinaz Safari Sanjani, Farhad Taghibakhsh, Craig S. Levin

Abstract– **This report characterizes a new set of SiPM (Silicon Photomultiplier) Detector Blocks for use in PET systems. This novel block consists of 9 arrays of 16-pixel SiPM detectors. Each pixel is 3mm by 3mm and the whole detector block is 46mm by 46mm by 133mm. the detector data is modified within each detector block and digital output comes out of each block. The digital output is then further processed in the coincidence board. The coincidence board is capable of supporting up to 16 individual detector blocks and connects to the computer via a fast USB cable.**

This report focuses on energy, time and uniformity characterization of two detector blocks. It determines the energy resolutions of individual pixels along with the global energy resolution of each block. The Coincidence Point Spread Function (CPSF) is also graphed and the average FWHM was calculated for the two detectors. The global energy resolution is calculated to be 18.1% and 19% for the detector blocks and the timing resolution is calculated to be 8.6 ns. Each pixel is multiplied by a normalization factor that makes all the photopeaks in the Detector be at the same energy. The energy of photopeaks of each pixel determines the uniformity of the two blocks. We used a 4 by 4 array of 13.1mm by 13.1 mm by 20 mm LYSO scintillator crystal pixelated at 3.1 mm by 3.1 mm to match the SiPM array pixels. The average FWHM of CPSF is calculated to be 1.90 ± 0.09 mm.

The modularity of these detector blocks and the digitized output signal along with good timing resolution, the reasonable energy resolution and the relative pixel uniformity make them suitable for nuclear medical imaging applications especially PET.

I. Introduction

The detector system analyzed in this report is the first modular and scalable system designed specifically for nuclear imaging applications. This technology is fully solid state, 4-way scalable and is used for fast scintillation applications. Employing SiPM (Silicon Photomultiplier) technology, these detectors need low power and low voltages to run. These detectors are built flexible enough to make them suitable for applications other than PET, such as Gamma Camera and SPECT.

This report focuses on energy, timing, uniformity, and spatial characterization of 2 individual photodetector blocks within this system. The detector head consists of 9 SiPM 4 by 4 arrays (making it suitable for temporal coincidence analysis). This passive detector head is connected within each block to readout electronics. The digital output of each block is further processed through the coincidence board. The arrays in each detector are connected together using a Scrambled Crosswire Readout technique. The coincidence board is capable of supporting up to 16 individual detector blocks and connects to the host computer via high speed USB connection. This layout is displayed in Fig. 1. The Coincidence Board is responsible for the configuration of each detector and the collecting of digitized event data for passing to the host computer.

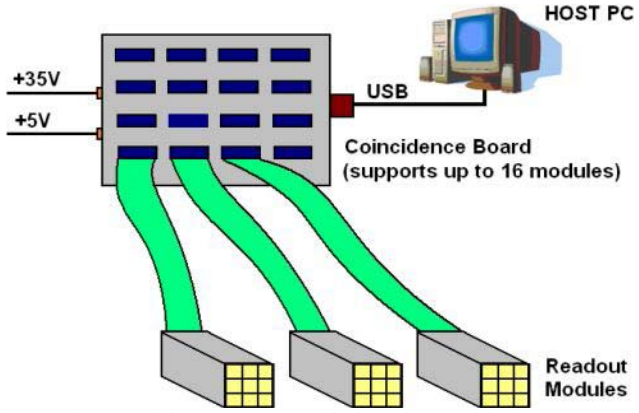

Fig. 1. Diagram of the components with three detector blocks connected to the coincidence board, and the board connected to the host computer via a fast USB cable.

II. Experiments, results and discussion

The uniformity and energy resolution portions of this report were based on the experimental setup shown in Fig. 2.

Manuscript submitted November 14, 2011.

This work is supported in part by in part by NSERC (Natural Sciences and Engineering Research Council of Canada) and Stanford Electrical Engineering Entrance Fellowship.

S. Safari Sanjani is with the department of Electrical Engineering, Stanford University, Stanford, CA 94305 USA (telephone: 650-391-6399, e-mail: sahinaz@stanford.edu).

F. Taghibakhsh, was with the department of Radiology, Stanford University, Stanford, CA 94305 USA. He is now with PerkinElmer Inc.. Santa Clara, CA USA (e-mail: farhadt@stanford.edu).

C. S. Levin is with the departments of Radiology, BioEngineering, Electrical Engineering, and Physics, Stanford University, Stanford, CA 94305 USA (e-mail: cslevin@stanford.edu).

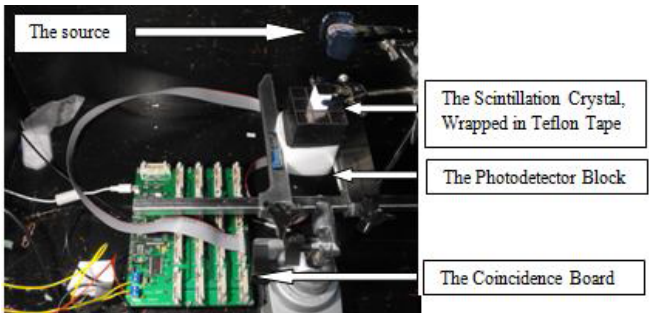

Fig. 2. The experiment setup for energy resolution and uniformity analysis, showing the detector block connected to the coincidence board, the 22Na source and the LYSO crystal array wrapped in Teflon.

In general, the detectors used are suitable only for applications involving fast scintillators. Therefore, we used a 4 by 4 array of 13.1mm by 13.1 mm by 20 mm LYSO scintillation crystal that consists of 16 pixels at 3.1 mm by 3.1 mm. Please note that the scintillation crystal was individually put on each array and the orientation of its pixels was visually aligned. The source was kept 4 cm away from the crystal with the same orientation with respect to the crystal at all times.

The experiment setup is based on powering the coincidence board with +35 and +5 and collecting data from the software related to the board.

Fig. 3 illustrates the global energy spectrum of the two detectors.

The energy resolution of detector 1 was calculated to be 18.1% . Among it pixels there is a range of 15.63% (Array 4, Pixel 2) to 34.85% (Array6, Pixel0) along with the standard deviation of 2.5. Detector 2 has the global energy resolution of 19%; with its pixels having an eneregy resolution that ranges between 18.61% (Array 2, Pixel 5) and 43.87% (Array 5, Pixel 3) with a standard deviation of 4.96.

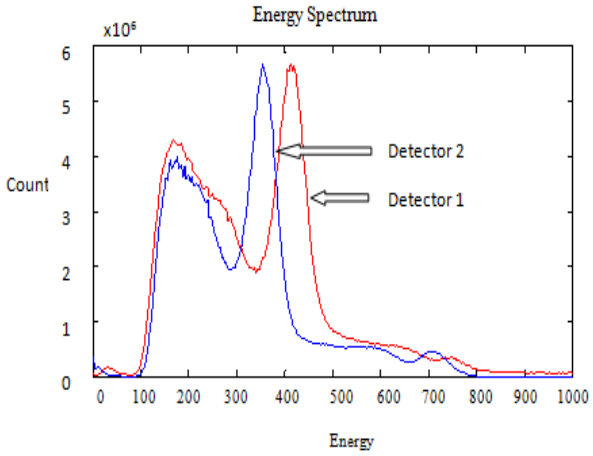

Fig. 3. The global energy spectrum of detectors 1 and 2 with the 511 keV photopeak energy resolutions of 19.0±2.5% and 18.1±5.0% FWHM, respectively. The global energy spectrum of each detector block was calculated by adjusting (in post-processing) the individual energy spectra of its pixels to have the same photopeak mean value.

We calculated the detectors gain uniformity maps based on the mean value of the Gaussian curve fitted to photopeaks of each pixel. The gain uniformity maps for both detectors are shown in Fig. 4. For detector 1, photopeaks vary from 177.8 to 355.4 ADC number with a mean value of 265.4 ADC number and a standard deviation of 25.7 (/μ = 9.7%). For Detector 2 this range is from 103.6 to 413.3 ADC number with a mean value of 320.1 ADC number and a standard deviation of 77.5 (/μ = 24.2%).

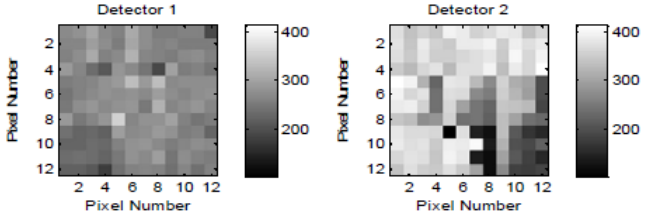

Fig. 4. Gain uniformity maps for both detectors (144 LYSO elements coupled one-to-one to 144 SiPM elements). This figure was obtained from the mean value of the Gaussian fit to the photopeak.

The flood images for both detectors are shown in Fig. 8. These images were constructed based on the number of counts within ± 1 of the photopeaks in each pixel. The number of counts for detector 1 ranges from 5503 to 7948 counts with a mean value of 6546 counts and a standard deviation of 510.2 (/μ = 7.8%). This range for detector 2 is evaluated to be 4696 to 9874 counts with a mean value of 6258 counts and a standard deviation of 1015.6 (/μ = 16.2%).

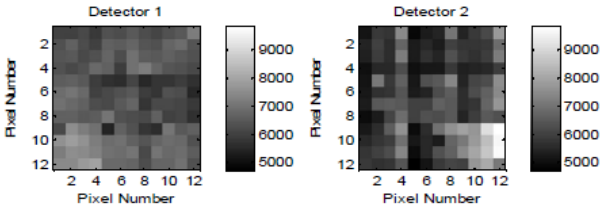

Fig. 5. Flood images of detectors 1 and 2. The images are formatted based on the counts within ± 1 of the mean photopeak of individual pixels

The coincidence time spectrum of a pair of coincidence pixels (pixel 9, array 7 of detector 1 and pixel 14, array 7 of detector 2) is shown in Fig. 9. The Gaussian curve fitted to the spectrum is also shown in the figure. This curve is used for finding the coincidence time resolution. For coincidence time spectrum, a window of 80 ns is used. A graph of these pixel locations on both detectors is shown in Fig. 6.

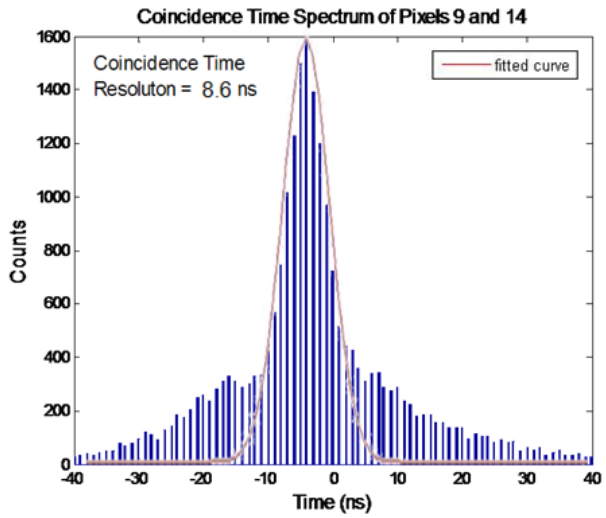

Fig. 6. The coincidence time spectrum of pixel 9, array 7, detector 1 and pixel 14, array 7, detector 2, and the Gaussian curve fitted to it to find the resolution. The coincidence time resolution is calculated to be 8.6 ns based on this graph.

The CPSF (Coincidence Point Spread Function) is graphed for four coincidence pairs in these detectors. Throughout this part of the experiment, the source was moved in steps of 300 micrometers. The Normalized CPSF graph is illustrated in Fig. 7.

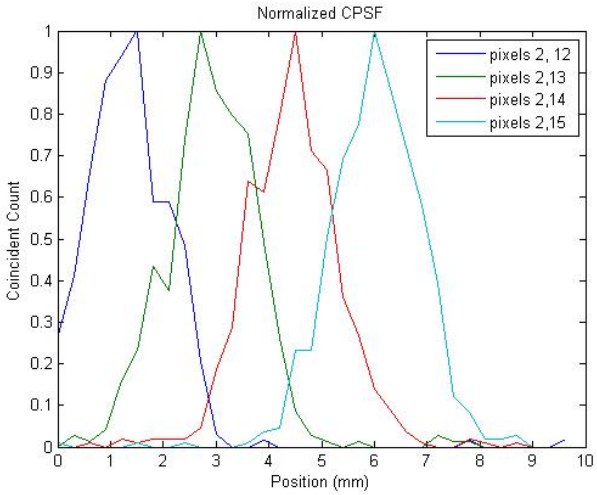

Fig. 7. Graph of normalized CPSF for better comparison of different SiPM pairs. The average FWHM of the normalized CPSF is 1.93 ± 0.29mm.

The FWHM of the four CPSF graphs range in 1.89 mm and 1.98 mm with a mean value of 1.93 ± 0.29mm.

III. Conclusions

In conclusion, the energy resolutions are calculated to be 18.1% and 19% with a timing resolution of 8.6 ns. Detector number 1 seems to be more uniform than the second detector. Based on the measurements and analysis of the report, we propose the use of this detector to acquire images for PET imaging systems.

Acknowledgment

The experiments in this report were done on Matrix9 Module provided and technically supported by SensL Technologies Ltd.